Measurement of Ocean Wave Directional Spectra Using Airborne HF/VHF Synthetic Aperture Radar: A Theoretical Evaluation

Alexander G. Voronovich and Valery U. Zavorotny, *Fellow, IEEE*

***Abstract*— Currently, images obtained with microwave synthetic aperture radars (SARs) are widely used for measuring directionality of ocean waves on a global and continuous scale. However, with all the advantages of the microwave SAR systems, the effectiveness of wave spectrum retrieval from SAR images is still debated. In this paper, we demonstrate how the directional spectrum of relatively long sea waves can be measured using aperture synthesis method in conjunction with relatively low radio frequencies (HF and VHF bands). This approach has advantages over HF ground-based radars used for ocean wave studies in coastal zones. In this paper, we theoretically evaluate this technique for the system mounted on aircraft. A favorable combination of the parameters for both ocean surface waves and HF electromagnetic waves allows an accurate analytical description of scattering from the sea surface based on the first approximation of the small perturbation method. In this case, scattered electromagnetic field becomes a linear functional of sea surface wave elevations. An analysis of the signal processing pertaining to this situation is presented, and a practical example is discussed. The proposed approach can be used even in the case when the radar platform is moving nonsteadily and/or along the curvilinear trajectory.**

***Index Terms*— HF radar, sea surface electromagnetic (EM) scattering, synthetic aperture radar (SAR).**

I. Introduction

THE spectrum of sea waves is an important parameter characterizing air–sea interactions and dynamics of the upper ocean. *In situ* instruments such as pitch-and-roll buoys provide frequency spectra, but their ability to accurately measure the directivity of sea waves is very limited. Over several decades, various remote sensing techniques using a wide range of the EM frequencies have been tested for more accurate measurements of the ocean wave directional spectra (see [1]–[10]). Since the late 1970s, it was recognized that synthetic aperture radar (SAR) images can provide useful information about sea surface waves (see [11], [12]). Satellite SARs allow acquiring global and continuous information about ocean waves from SAR imagery. However, with all technological advances achieved in the satellite microwave SAR ocean imagery, the effectiveness of the wave spectrum retrieval from SAR images is still debated (see [13], [14]).

Manuscript received September 22, 2016; revised December 19, 2016; accepted January 19, 2017. Date of publication March 2, 2017; date of current version May 19, 2017.

The authors are with the Earth System Research Laboratory, National Oceanic and Atmospheric Administration, Boulder, CO 80305 USA (e-mail: alexander.voronovich@noaa.gov; valery.zavorotny@noaa.gov).

Digital Object Identifier 10.1109/TGRS.2017.2663378

The physical mechanism of the microwave SAR imaging of ocean waves is well studied in the literature [11], [12]. At the same time, it was long recognized that due to the nonuniform motion of the scatterers on the time-dependent sea surface, the SAR imaging process is, in general, strongly nonlinear [12]. Two most important mechanisms are involved in the ocean wave microwave SAR imaging: 1) the radar cross section modulation by the distribution of Bragg resonant ripples and 2) the distorting effect of the orbital motion of the water particles associated with the long ocean surface waves known as "velocity bunching" (see [12]). As a result, the retrieval of sea wave amplitudes from the SAR data represents a difficult nonlinear problem.

Since the interpretation of standard microwave SAR images of the sea surface in terms of wave directional spectra encounters difficulties mentioned above, other approaches for measuring sea wave spatial spectra were also tried. For example, an airborne scanning radar altimeter (and its successor, Wide Swath Radar Altimeter) was used successfully in the past to map wave directional spectra, but this instrument is quite unique [8]–[10], [15]. Also, images obtained with shipborne real aperture radars have been used for the determination of ocean wave directionality in the vicinity of a ship, but the spatial coverage of such systems is rather limited [7].

Apart from the microwave sensors, the HF sensors using signals with meter, or tens of meters, wavelength are capable of measuring wave directional spectra using resonant Bragg scattering by long surface gravity waves without the abovementioned nonlinearity problems. Indeed, sea surface waves have rather limited RMS elevations (not exceeding the order of meters), and for not too strong winds they have small slopes. Under these circumstances, it seems expedient to use longer radio waves with wavelength exceeding RMS surface elevations. For such waves, scattering is due to Bragg resonant mechanism, which was first confirmed experimentally by Crombie [16] who observed Doppler spectra of the 13 MHz radio signals scattered from the rough sea surface using a coastal installation. Later Barrick [17] (see also [1]) introduced a theoretical model for the HF sea-echo Doppler spectrum, which relates it to the ocean wave directional spectrum and the surface current velocity. Such a theoretical model is particularly simple for sufficiently long radio waves possessing a small Rayleigh parameter when the small perturbation method is applicable and the scattered EM field becomes a linear functional of wave elevations. These advances led to

development of coastal HF radar systems for the remote sensing of sea-surface parameters. Since then, they have become available for producing current maps and retrieving wave directional information [2]–[6]. Also, the theoretic models of the HF ocean wave scattering became more advanced (see [18]). Among the deficiencies of such HF systems are a spatial coverage, which is limited to coastal areas, and a rather modest spatial resolution.

Although coastal (or ship-borne) HF "*non-SAR*" radar systems have been used for this purpose long ago, they have limitations with respect to coverage and resolution. To obtain high azimuthal directivity, rather large and expensive antenna arrays (such as WERA) are employed in HF coastal radar systems [5]. Here, we propose to utilize the synthetic aperture concept in the HF/VHF band for measurements of ocean wave directional spectra from aircraft, which should significantly reduce limitations typical for the coastal HF radar systems.

The early algorithms of SAR signal processing relied on the fast Fourier transformation (FFT). If radar is moving nonsteadily and/or along the curvilinear trajectory, and/or the scene is not stationary, then an FFT is not quite adequate, and resolution might degrade significantly. The modern high-resolution SAR processing is still using the FFT at different stages of signal processing but it is not limited to it (see [19]). In terms of SAR signal processing, our approach invokes a time-domain consideration, which makes it similar to time-domain back-projection (TDBP) algorithms proposed in [20] and [21], which at present have become computationally feasible and rather popular. Those algorithms are very flexible in treating cases when the radar platform is moving nonsteadily and/or along the curvilinear trajectory.

It should be stressed here that the proposed technique does not intend to produce any SAR type imagery of the overflying ocean scene. The received signal will be processed in such a way that the output will yield the wave directional spectra for some spatial area surveyed by the aircraft. In contrast to microwave SAR systems, in this case, the surface waves of a particular wavelength are directly sensed by appropriate radio waves in the HF/VHF band, roughly by a double wavelength.

Some similarity exists between the suggested approach and the technique, which employs shipborne high frequency surface wave radar (HFSWR) for measuring wind direction [22]. Namely, when scattering is measured from a moving ship, signals coming from different directions experience different Doppler shift, which is proportional to the cosine of the angle between ship velocity and direction of propagation of Bragg scattering waves. For ship-mounted radar, scattering always proceeds under very small grazing angle, and the wavelength of the Bragg scattering waves is two times shorter than the electromagnetic wavelength and is practically fixed. In the case of aircraft, however, the wavelength of Bragg scattering waves depends on the varying grazing angle between aircraft and various portions of the scattering scene. Taking advantage of this fact allows one to retrieve the wavenumber dependence of a sea wave spectrum within certain limits.

The approach considered here and a standard SAR processing have both similarities and differences. The similarity is in using of broadband signals and antenna aperture synthesis. The differences (besides those already discussed above) are: 1) modeling of EM sea surface scattering using the first-order perturbation method, which is not applicable in the case of microwave SAR and terrain scenes, but is adequate for relatively long EM waves and a sea surface and 2) direct interpretation of measurements in terms of sea surface spectra.

To sum up, this paper presents a theoretical development of the method, which uses HF or VHF EM waves in conjunction with the aperture synthesis approach for the measurement of ocean wave directional spectra for wavelengths starting from 5 to 10 m and longer. It can be viewed as a generalization of the coastal HF radar technique for the case of a fast-moving airborne platform with a synthesized rather than a real aperture. It is important to stress that for the aircraft implementation, the proposed technique is not limited to a straight and uniform movement of the platform. It can be used for platforms that are moving nonuniformly along curved trajectories including circular ones. This also can be very useful for a better sampling of localized scenes and longer coherent integration times. Extending this technique to space-borne platforms is, in principle, possible, but it is a challenging problem because of adverse ionospheric effects, limited statistics, and a limited set of directions from which a given ocean area can be illuminated (to this point, see also Section III).

We avoid discussing the technical implementation of the proposed method here. However, we can direct interested readers to publications on existing airborne HF SAR systems, which can be used as a prototype for our system. For example, SARs working in HF frequencies have become attractive for application in reconnaissance through foliage, vegetation and biomass measurements, Arctic ice studies, etc. [23]–[25]. Let us emphasize that in our approach, a transmitting/receiving antenna with a broad radiation pattern is employed, which must be known in advance. This might present a problem that needs to be addressed in the practical implementation of this technique.

Our approach is outlined in Section II. The discussion of results is presented in Section III. The derivation of the expression for the scattered field can be found in Appendix A.

II. Outline of the Approach

In Section I, we pointed out that our approach has much in common with the time-domain aperture synthesis method, which is based on a coherent summation of signals received by small subapertures sequentially occupying various locations of the virtual aperture. To start with a derivation of the expression for the received signal, we need to describe the scattered field. For this, we will use a general expression (A21) obtained in Appendix A for the complex amplitude of the monochromatic scattered field measured at the point $(\vec{r}_0, z_0)$ at the moment of time t_0.

We will assume that the scattered field Ψ is measured at a set of points $(\vec{r}_n, z_n)$ at different moments of time t_n, where $n = -N, \ldots, N$ is a radar pulse index of $2N + 1$ pulses altogether (see Fig. 1). Let $\Psi_n(\omega)$ is a complex amplitude originating from the Fourier transformed time series of the nth transmitted and received pulses after "pulse compression",

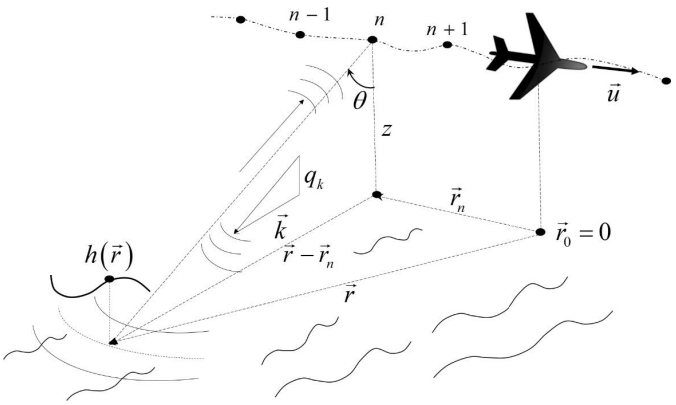

Fig. 1. Illustration of the measurement geometry. Indices $n-1, n, n+1, \ldots$ indicate antenna locations from which radar pulses were sent and received.

i.e., the ratio of the complex amplitudes of the received, $\Psi_{\rm rec}$, and transmitted, Ψ_{tr}, pulses

$$\Psi_n(\omega) = \frac{\Psi_{\rm rec}(\vec{r}_n, z_n, t_n; \omega)}{\Psi_{tr}(n,\omega)} = \frac{\Psi_{\rm rec}(\vec{r}_n, z_n, t_n; \omega)[\Psi_{tr}(n,\omega)]^*}{|\Psi_{tr}(n,\omega)|^2}. \quad (1)$$

It is assumed that we are dealing with a broadband signal, and that none of its frequency components within a certain band turns into zero: $|\Psi_{tr}(n,\omega)|^2 \neq 0$. Values $\Psi_n(\omega)$ are thus known from measurements; they are actually used in certain SAR applications. Since we will be performing the coherent processing, all pulses should be processed in the same time frame. In particular

$$\Psi_{tr}(n,\omega) = \Psi_{tr}(0,\omega)e^{i\omega t_n}. \quad (2)$$

We will assume that the time interval of measurements is not too long so the amplitudes of surface waves can be considered constant. In Appendix A, the following expression for $\Psi_n(\omega)$ was obtained [see (A21)]:

$$\Psi_n(\omega) = \int d\vec{\xi} e^{i\vec{\xi}\vec{r}_n + 2iz_n q_{\xi/2}(\omega)} D(\vec{\xi},\omega) \times [a(\vec{\xi})e^{-if(\xi)t_n} + a^*(-\vec{\xi})e^{if(\xi)t_n}] \quad (3)$$

where $\vec{\xi}$ is the wave vector of a surface gravity wave and $a(\vec{\xi})$ and $f(\xi) = \sqrt{g\xi}$ are its complex amplitude and circular frequency, respectively. In (3), $q_{\xi/2}$ is a vertical projection of the wave vector of the plane wave selected due to the Bragg-scattering mechanism from the superposition of plane waves radiated by the source. Function D represents the radiation pattern of the antenna, and it also accounts for the spherical divergence and the intensity of Bragg scattering (see Appendix A for details).

In (3), the dependences of factors $q_{\xi/2}$ and D on frequency ω are explicitly indicated; in Appendix A ω was considered as a parameter.

Equation (3) represents a linear set inverting which one can principally infer unknown surface wave amplitudes $a(\vec{\xi})$. In practical cases, the number of available frequencies can be of the order of 10^4 or even larger; the number of pulses can be of the order of 10^3–10^4. An extremely large number of resulting equations makes a brute-force solution of the linear set impractical. However, as it is explained below, the summation of pulses with proper phase factors with respect to index n and the Fourier transform of the result with respect to the frequency will collapse the kernel of the integrand in the RHS of the resulting equation into a function with a narrow support on the $\vec{\xi}$-plane, which makes these equations much easier to solve by iterations. Moreover, we are interested in statistically averaged squares of amplitudes of the sea surface waves rather than in individual realizations of the wave field. Such an averaging results in some simplifications of final expressions.

The transformations of (3), which will be presented below, are similar to two main steps of a standard SAR processing, namely selection of signals coming from certain directions by calculating Doppler spectrum and selection of signals coming from a certain distance by time gating. However, HF SAR imaging of the sea surface is not our goal, and the suggested below processing scheme is technically different as compared to standard SAR processing methods; it can be considered as a version of "back projection" approach [21]. Note that our processing does not rely on the trajectory of the radar being a straight line; this might be an advantage when integration time increases, and/or circular flights are used.

By making use of $\Psi_n(\omega)$, let us calculate the following function:

$$F(\vec{k}) = \frac{1}{\pi^{1/2}\Omega}\int d\omega e^{-\frac{(\omega-\omega_0)^2}{\Omega^2}} \frac{p}{\pi^{1/2}N} \times \sum_{n=-N}^{N} \Psi_n(\omega) e^{-i\vec{k}\vec{r}_n - 2iz_n q_{k/2}(\omega) + if(k)t_n - p^2n^2/N^2}. \quad (4)$$

Substituting representation (3) into (4), one obtains

$$F(\vec{k}) = \int [T_+(\vec{k},\vec{\xi})a(\vec{\xi}) + T_-(\vec{k},\vec{\xi})a^*(-\vec{\xi})] \quad (5)$$

where

$$T_+(\vec{k},\vec{\xi}) = \frac{1}{\pi^{1/2}\Omega}\int d\omega D(\vec{\xi},\omega)e^{-\frac{(\omega-\omega_0)^2}{\Omega^2}} \times \frac{p}{\pi^{1/2}N}\sum_{n=-N}^{N} \times e^{i(\vec{\xi}-\vec{k})\vec{r}_n - 2iz_n(q_{\xi/2}(\omega)-q_{k/2}(\omega)) + i(f(k)-f(\xi))t_n - p^2n^2/N^2} \quad (6)$$

and $T_-(\vec{k},\vec{\xi})$ differs from $T_+(\vec{k},\vec{\xi})$ defined by (6) only by the plus sign in front of $f(\xi)$ in the exponent. Parameter ω_0 in the first exponent in (6) is a center (angular) frequency of the transmitted signal and parameter Ω is supposed to be somewhat less than the frequency bandwidth so that contributions from terminal frequencies in (6) are withered away. Thus, parameter Ω is an effective frequency bandwidth of our processing.

Let us first consider the meaning of the sum in (4). As it is clear from (6), that exponential factors in the sum in (4) are chosen such that phase shifts due to varying locations and times of the measurements will be compensated in all pulses for the Bragg-scattered waves with $\vec{\xi} = \vec{k}$. For this reason, one might expect function $T_+(\vec{k},\vec{\xi})$ to have a maximum around

point $\vec{\xi} = \vec{k}$ on the $\vec{\xi}$-plane. Similar to the exponential factor $\exp(-(\omega-\omega_0)^2/\Omega^2)$, the factor $\exp(-p^2n^2/N^2)$ withers away the contribution from terminal pulses; thus, parameter p should somewhat exceed unity. Both smoothing factors are introduced to remove undesirable side lobes in functions $T_\pm(\vec{k},\vec{\xi})$ on the $\vec{\xi}$-plane making their support more compact.

As it will become more evident in what follows, the summation over pulses in (4) and (6) is similar to the Doppler frequency filtering and the sum in (6) has in fact maximum not for $\vec{\xi} = \vec{k}$ only, but for all Bragg-scattered waves having close Doppler frequencies. To reduce dimensionality of the support of functions $T_\pm(\vec{k},\vec{\xi})$ on the $\vec{\xi}$-plane, integration over ω in (4) is added. This integration selects the Bragg-scattered waves that have close propagation time toward the sea surface and back what as we will also see below is equivalent to selection of waves with $|\vec{\xi}| = |\vec{k}|$.

In the case of a spatially homogeneous statistical ensemble of surface waves, one has

$$\langle a(\vec{k})a(\vec{k}')\rangle = 0,\ \langle a(\vec{k})a^*(\vec{k}')\rangle = \frac{1}{2}W(\vec{k})\delta(\vec{k}-\vec{k}') \tag{7}$$

where $W(\vec{k})$ is a directional spectrum of surface waves with usual normalization

$$\langle h^2\rangle = \int W(\vec{k})d\vec{k}. \tag{8}$$

Now, from (5), one finds

$$\langle |F(\vec{k})|^2\rangle = \frac{1}{2}\int [|T_+(\vec{k},\vec{\xi})|^2 W(\vec{\xi}) + |T_-(\vec{k},\vec{\xi})|^2 W(-\vec{\xi})]d\vec{\xi}. \tag{9}$$

Equation (9) can be considered as a linear integral equation with respect to the wave spectrum W.

In the general case of arbitrary trajectory, bandwidth, and antenna radiation patterns, functions $T_\pm\left(\vec{k},\vec{\xi}\right)$ can be calculated numerically according to (6). To obtain insight into their structure we will consider a particular case of an airborne platform moving uniformly with velocity $\vec{u}$ along a straight horizontal path and set: $t_n = n\tau$, $\vec{r}_n = \vec{u}t_n$, $z_n = z_0$. Let us also assume the case of narrowband pulses

$$\Omega \ll \omega_0. \tag{10}$$

Then, we obtain

$$T_+(\vec{k},\vec{\xi}) = \frac{D(\vec{\xi},\omega_0)}{\pi^{1/2}\Omega}\int d\omega e^{-\frac{(\omega-\omega_0)^2}{\Omega^2}} e^{-2iz_0(q_{\xi/2}(\omega)-q_{k/2}(\omega))} \times \frac{p}{\pi^{1/2}N}\sum_{n=-N}^{N} e^{i(\vec{\xi}-\vec{k}+f(k)-f(\xi))n\tau - p^2n^2/N^2} \tag{11}$$

where the weak dependence of function $D(\vec{\xi},\omega)$ on frequency within narrow frequency band was neglected.

For sufficiently small τ, the sum in (11) can be replaced by a corresponding integral, which we will extend to infinite limits and find

$$\frac{p}{\pi^{1/2}N}\sum_{n=-N}^{N} \times \exp\{i[(\vec{\xi}-\vec{k})\vec{u} + f(k) - f(\xi)]n\tau - p^2n^2/N^2\} = \exp\left\{-\left(\frac{N\tau}{2p}\right)^2[(\vec{\xi}-\vec{k})\vec{u} + f(k) - f(\xi)]^2\right\}. \tag{12}$$

One can see that the expression in the bracket represents a difference of Doppler frequencies of the Bragg-scattered waves with horizontal projections of the wave vectors equal to $\vec{\xi}$ and $\vec{k}$. If one neglects the presence of the term $f(k)-f(\xi)$ in the right-hand side of (12), the bracket will turn to zero along the straight line that passes through vector $\vec{k}$ in the direction perpendicular to vector $\vec{u}$: $(\vec{\xi}-\vec{k})\vec{u} = 0$. The width of the ridge around the line nullifying the bracket in (12) is inversely proportional to the total coherent integration time, $2N\tau$. When performing integration over ω in (11) under condition (10) we will approximate the expression in the exponent by the first two terms of the power expansion with respect to $(\omega-\omega_0)$:

$$q_{\xi/2}(\omega) - q_{k/2}(\omega) \approx q_{\xi/2}(\omega_0) - q_{k/2}(\omega_0) + \frac{\xi^2-k^2}{4}\frac{\omega_0}{c^2}\frac{1}{q_{\xi/2}(\omega_0)+q_{k/2}(\omega_0)} \times \frac{(\omega-\omega_0)}{q_{\xi/2}(\omega_0)\,q_{k/2}(\omega_0)}. \tag{13}$$

As we will see shortly, for sufficiently large z_0 one has $\xi \approx k$. For this reason, we can simplify (13) and obtain

$$q_{\xi/2}(\omega) - q_{k/2}(\omega) \approx q_{\xi/2}(\omega_0) - q_{k/2}(\omega_0) + \frac{k\omega_0(\xi-k)}{4c^2q_{k/2}^3(\omega_0)}(\omega-\omega_0). \tag{14}$$

In this approximation one finds

$$\frac{1}{\pi^{1/2}\Omega}\int d\omega e^{-\frac{(\omega-\omega_0)^2}{\Omega^2}} e^{-2iz_0(q_{\xi/2}(\omega)-q_{k/2}(\omega))} = e^{-2iz_0(q_{\xi/2}(\omega_0)-q_{k/2}(\omega_0))} \times \exp\left[-\left(\frac{\Omega z_0k^2\omega_0}{4c^2q_{k/2}^3(\omega_0)}\right)^2\left(\frac{\xi-k}{k}\right)^2\right]. \tag{15}$$

Let us introduce incidence angle θ instead of parameters $k/2$, $q_{k/2}$ in the coefficient of the second exponent in the right-hand side of (15) according to the relations

$$k = 2\frac{\omega_0}{c}\sin\theta, \quad q_{k/2} = \frac{\omega_0}{c}\cos\theta. \tag{16}$$

As a result, (11) takes the form

$$T_+(\vec{k},\vec{\xi}) = e^{-2iz_0(q_{\xi/2}(\omega_0)-q_{k/2}(\omega_0))}D(\vec{\xi},\omega_0) \times \exp\left\{-\left(\frac{\Omega z_0}{c}\frac{\sin^2\theta}{\cos^3\theta}\right)^2\left(\frac{\xi-k}{k}\right)^2 - \left(\frac{N\tau}{2p}\right)^2[(\vec{\xi}-\vec{k})\vec{u} + f(k) - f(\xi)]^2\right\}. \tag{17}$$

The expression for $T_-(\vec{k},\vec{\xi})$ follows from (17) after replacing $f(k)-f(\xi)$ by $f(k)+f(\xi)$.

One can see from (17) that the relative width of functions $T_{\pm}(\vec{k},\vec{\xi})$ on the $\vec{\xi}$-plane with respect to modulus of vector $\vec{\xi}$ for small and moderate incidence angles is of the order of

$$\frac{\xi-k}{k}\sim\frac{c}{\Omega z_0}\frac{1}{\sin^2\theta}. \tag{18}$$

This relation determines the characteristic value of the minimal incident angle for which kernels $T_{\pm}(\vec{k},\vec{\xi})$ are still narrow enough

$$\sin\theta_{\min}\sim\left(\frac{c}{\Omega z_0}\right)^{1/2}. \tag{19}$$

It is interesting that, as the simple geometry shows, practically the same restriction on the incidence angle follows from the necessity to remove specularly reflected pulse by time gating. The wavelength of the longest surface wave $\lambda_{\max}$, which can be sensed by this approach, correspondingly reads

$$\lambda_{\max}=\frac{2\pi}{k_{\min}}\sim\frac{\pi c}{\omega_0}\frac{1}{\sin\theta_{\min}}=\frac{\pi c}{\omega_0}\left(\frac{\Omega z_0}{c}\right)^{1/2}. \tag{20}$$

The width of functions $T_{\pm}(\vec{k},\vec{\xi})$ on the $\vec{\xi}$-plane with respect to azimuthal angle φ (calculated with respect to vector $\vec{u}$) follows from the second bracket in the exponent in (17) and reads

$$\delta\varphi\sim\frac{1}{\pi}\frac{2\pi}{k}\frac{p}{N\tau u\sin\varphi}=\frac{1}{\pi}\frac{p}{\sin\varphi}\frac{\lambda_s}{N\tau u}. \tag{21}$$

As expected, the main parameter here is the ratio of the wavelength of surface wave $\lambda_s=2\pi/k$ to the length of synthetic aperture $2N\tau u$.

Note, that if for function $T_{+}(\vec{k},\vec{\xi})$ both brackets in the exponent in (17) turn to zero at $\vec{\xi}=\vec{k}$, for function $T_{-}(\vec{k},\vec{\xi})$ the zero of the second bracket

$$(\vec{\xi}-\vec{k})\vec{u}+f(k)+f(\xi)=0 \tag{22}$$

is located at a slightly shifted direction; the shift is small since the phase velocity of surface waves $f(k)/k$ is usually significantly less than speed of the airborne platform u. Let us designate a corresponding vector as $\vec{k}_f$. If the total coherent integration time $2N\tau$ significantly exceeds a period of the surface wave $1/f(k)$, corresponding maxima at the points $\vec{k}$ and $\vec{k}_f$ will not overlap, and contributions from the surface waves propagating toward and away from the radar [the first and the second terms in (9)] can be principally separated.

If parameters $\Omega z_0/c$ and $Nu\tau/\lambda_s$ are large, and the supports of functions $T_{\pm}(\vec{k},\vec{\xi})$ are correspondingly small enough, variations of spectrum Wwithin the supports can be neglected in the first approximation. Note that function T_{+}specified in (17) for a given $\vec{k}$ has, in fact, two maxima on the $\vec{\xi}$-plane. These maxima which we denote as $\vec{k}$ and $\vec{k}'$ are symmetrically located on both sides of vector $\vec{u}$. The same pertains to the second term of (9). As a result, (9) can be approximately represented as

$$\begin{aligned}\langle|F(\vec{k})|^2\rangle=&\frac{1}{2}\sum_{\vec{\xi}=\vec{k},\vec{k}'}W(\vec{\xi})\int|T_{+}(\vec{k},\vec{\xi}+\Delta\vec{\xi})|^2d\Delta\vec{\xi}\\&+\frac{1}{2}\sum_{\vec{\xi}=\vec{k}_f,\vec{k}'_f}W(-\vec{\xi})\int|T_{-}(\vec{k},\vec{\xi}+\Delta\vec{\xi})|^2d\Delta\vec{\xi}\end{aligned} \tag{23}$$

where the integrals over $\Delta\vec{\xi}$ proceed over small areas around the origin. The presence of double sums in (23) leads to a certain ambiguity, which is briefly addressed in the next section.

If the direction of vector $\vec{k}$ is not too far away from the wind direction, then $W(-\vec{k})\ll W(\vec{k})$. Let us assume also that the radar antenna pattern although broad dominates nevertheless in the direction $\vec{k}$ as compared to $\vec{k}'$: $D(\vec{k},\omega_0)\gg D(\vec{k}',\omega_0)$. Then, only one term in (23) survives and we obtain

$$W(\vec{k})\approx 2\langle|F(\vec{k})|^2\rangle\left(\int|T_{+}(\vec{k},\vec{\xi})|^2d\vec{\xi}\right)^{-1}. \tag{24}$$

This solution can be considered as a first approximation of an iterative solution of the linear equation (9). Next iterations will take into account the three neglected terms in the RHS of (23), as well as variations of the spectrum within the supports of functions $T_{\pm}(\vec{k},\vec{\xi})$.

III. Discussion of the Results

In this paper, we theoretically demonstrated the feasibility of measuring the directional spectrum of ocean surface waves by HF/VHF radar with synthetic aperture in a monostatic configuration. RMS elevations of ocean waves for not too strong winds do not exceed a few meters, and the wavelength of the carrier in the range of 10–20 m might be a reasonable choice. The Bragg wavelength increases without a limit when the look direction approaches the nadir; for this reason, the long-wave part of the ocean wave spectrum can be retrieved. The shortest surface waves for which the spectrum can be principally measured by this approach correspond to roughly half of the electromagnetic wavelength calculated at the center of the frequency band. If the length of synthetic aperture $2u\tau N$ significantly exceeds the wavelength of surface waves, the angular resolution will be rather high. This is the main advantage of the proposed approach.

Let us make some numerical estimates. Let the carrier frequency be $\omega_0\sim 2\pi\cdot 20$ MHz, which corresponds to the wavelength of the electromagnetic wave $\lambda_{EM}=15$ m. The Rayleigh parameter will be reasonably small for not too strong winds so that the first-order approximation of the small perturbation method should be adequate. Let us also assume $z_0\sim 2\cdot 10^3$ m and $\Omega\sim 2\pi\cdot 2$ MHz. Then from (20), one finds $\lambda_{\max}\sim 70$ m, which seems to be enough for moderate winds. $\lambda_{\max}$ can be increased by increasing z_0 and/or Ω. The smallest wavelength of the surface waves that can be sensed by the Bragg scattering mechanism will be in this case $\lambda_{\min}=\lambda_{\mathrm{EM}}/2=7.5$ m. If the length of synthetic aperture $2N\tau u=2$ km, according to (21) the angular resolution will be of the order of a few degrees for surface waves of the order of $\lambda_s\sim 70$ m, and for shorter waves the angular resolution will be even finer.

It is worthwhile to mention that, in fact, this estimate of angular resolution corresponds to the first-order solution (24). Further iterations of the basic equation (9) will increase the angular resolution even further. For an iterative solution to be stable the width of the support of functions $T_{\pm}(\vec{k},\vec{\xi})$ should not be too large as compared to the scale on which spectrum $W(\vec{k})$ varies; otherwise, the solution may become inaccurate if SNR

is not high enough. Assuming the aircraft speed being of the order of $u \sim 150$ m/s, one finds that the coherent integration time required to create a synthetic aperture of 2-km length will be $\sim$13 s which is twice as much as a period of 70-m length surface wave. Thus, surface waves propagating toward and away from the radar could be resolved. By reducing the carrier frequency ω_0, one can probe the case of higher winds characterized by larger amplitudes and wavelengths of surface waves.

Since the resolutions given by (18) and (21) increase with increase of elevation z_0 and synthetic aperture length $2N\tau u$, it is interesting to consider a possibility to use a space borne platform for measurements. However, one has to have in mind possible obstacles for doing this. First, ionospheric effects should be taken into account. Second, there might be a problem in collecting enough realizations to perform statistical averaging, since the platform quickly passes over the areas where the surface wave fields can be considered as statistically homogeneous. Third, probably the sphericity of the Earth has to be taken into account. As far as ionospheric effects go, assertions can be found in the literature that destructive ionospheric effects can be successfully compensated for by means of adaptive 2-D processing of received signals [26], [27].

Another interesting application maybe an attempt to retrieve individual realizations of the sea surface based on (5) without statistical averaging. In this case, however, the oscillating factor in front of the function D in (17) has to be taken into account. To reduce its negative impact, one has to increase the width of the frequency band and make it comparable to the carrier. Another problem might be the fast variation of phases of different waves within the support of $T_{\pm}$ functions. This possibility requires a separate investigation. If successful, one might try to mitigate the defects of microwave SAR caused by orbital velocities of longer waves by taking into account time-dependent topography of these waves retrieved from HF SAR measurements.

As (21) shows, angular resolution decreases in the directions close to the direction of velocity $\vec{u}$. To make angular resolution uniform, one might try to use measurements from a few different directions of $\vec{u}$. This will also help to resolve the ambiguity associated with two maxima of functions $T_{\pm}$ and allow one an internal check of the procedure, since the retrieved spectrum $W(\vec{k})$ should not, of course, depend on $\vec{u}$.

Note that in view of a relatively large wavelength of electromagnetic waves, keeping track of the antenna position with $\lambda_{EM}/10 \sim 1.5$ m accuracy during aperture synthesis should not be too difficult.

An extension of the approach presented in this paper can be also formulated for the case of bistatic VHF SAR. This type of SAR was demonstrated recently in [28].

APPENDIX A

Let us introduce some notations. Let $\vec{r}, \vec{r}_0$, be horizontal and z, z_0 vertical coordinates of the observation point, and source location, respectively (z-axis is directed upward)

$$R = \sqrt{(\vec{r} - \vec{r}_0)^2 + (z - z_0)^2}, \tag{A1}$$

$\vec{k}$ is a horizontal projection of the wave vector of a plane wave, and

$$q_k = \sqrt{(\omega/c)^2 - k^2} \tag{A2}$$

is a vertical projection of the wave vector. A well-known representation of the field of an omnidirectional point source of a unit amplitude in the form of a superposition of plane waves reads

$$\frac{e^{i(\omega/c)\,R}}{(\omega/c)R} = \frac{i}{2\pi}\frac{c}{\omega}\int \frac{d\vec{k}}{q_k} e^{i\vec{k}(\vec{r}-\vec{r}_0)+iq_k|z_0-z|}. \tag{A3}$$

Correspondingly, the field Ψ_{tr} propagating downward due to a transmitting antenna with a radiation pattern $d_{tr}(\vec{k})$ located at a point $(\vec{r}_0, z_0)$ can be represented as follows:

$$\Psi_{tr}(\vec{r}, z) = \frac{i}{2\pi}\frac{c}{\omega}\int d\vec{k}_0 d_{tr}(\vec{k}_0)\, q_{k_0}^{-1/2} e^{-i\vec{k}_0\vec{r}_0+iq_{k_0}z_0} \times q_{k_0}^{-1/2} e^{i\vec{k}_0\vec{r}-iq_{k_0}z} \tag{A4}$$

where the integration variable $\vec{k}$ is replaced by $\vec{k}_0$. If the incident field is calculated in the far zone, the principle of stationary phase can be applied to the integral in (A4). As a result one obtains an isotropic spherical wave from the left-hand side of (A3) multiplied by $d_{tr}(\vec{k}^{(st)})$. Here, $\vec{k}^{(st)} = \omega/c\vec{n}$ is a stationary point, with $\vec{n}$ being the horizontal projection of the unit vector directed from the transmitting antenna toward the observation point. Using this relationship one can easily represent function $d_{tr}(\vec{k}_0)$ in terms of any other parameters characterizing the antenna radiation pattern and gain. Note that due to the normalization employed in (A3), the radiation pattern $d_{tr}(\vec{k}_0)$ is a dimensionless function.

The last factor in (A4) represents an individual plane wave propagating downward. It is convenient to represent the scattered field in terms of scattering amplitude, which is defined as follows. Let the incident field is a plane wave from (A4). Then the expression for the total field ψ at the point $\vec{r}$, $z > 0$ reads

$$\psi = q_{k_0}^{-1/2} e^{i\vec{k}_0\vec{r}-iq_0z} + \psi_{sc} \tag{A5}$$

where

$$\psi_{sc} = \int q_k^{-1/2} e^{i\vec{k}\vec{r}+iq_kz} S(\vec{k}, \vec{k}_0)\, d\vec{k} \tag{A6}$$

represents the scattered field as a superposition of plane waves propagating upward, and $S(\vec{k}, \vec{k}_0)$ is a scattering amplitude of the plane wave with the horizontal projection of the wave vector $\vec{k}_0$ into a plane wave with the horizontal projection of the wave vector $\vec{k}$ [29]. Here, scalar ψ represents an EM wave of certain polarization. Using a superposition principle, one finds the received field due to the incident field from (A4) as follows:

$$\Psi_{\text{rec}}(\vec{r}, z) = \frac{i}{2\pi}\frac{c}{\omega}\int d_{tr}(\vec{k}_0)\, q_{k_0}^{-1/2} e^{-i\vec{k}_0\vec{r}_0+iq_{k_0}z_0} \times \int d\vec{k} d_{\text{rec}}(\vec{k})\, q_k^{-1/2} e^{i\vec{k}\vec{r}+iq_kz} S(\vec{k}, \vec{k}_0) \tag{A7}$$

where similarly to the case of incident field we have introduced the radiation pattern of the receive antenna $d_{\text{rec}}(\vec{k})$. If the wavelength of the incident wave significantly exceeds

elevations $h(\vec{r})$ and the latter have small slopes then the small perturbation method applies and the expression for the scattering amplitude reads [29]

$$S(\vec{k},\vec{k}_0) = V_F(\vec{k}_0)\,\delta(\vec{k}-\vec{k}_0) - 2i\,(q_k q_{k_0})^{1/2} B(\vec{k},\vec{k}_0)\,\hat{h}(\vec{k}-\vec{k}_0) \quad \text{(A8)}$$

where

$$V_F(\vec{k}_0) = B(\vec{k}_0,\vec{k}_0) \quad \text{(A9)}$$

is the Fresnel reflection coefficient from the plane surface without roughness, and $\hat{h}(\vec{k})$ is the roughness elevation spectrum

$$\hat{h}(\vec{k}) = \int e^{-i\vec{k}\vec{r}} h(\vec{r})\,\frac{d\vec{r}}{(2\pi)^2}. \quad \text{(A10)}$$

The first term in (A8) represents the specularly reflected field and the second term describes Bragg scattering. $B(\vec{k},\vec{k}_0)$ in (A8) is a dimensionless regular function; for the case of VV polarization it is

$$B(\vec{k},\vec{k}_0) = \frac{(\varepsilon-1)\left(q_k^{(\varepsilon)} q_{k_0}^{(\varepsilon)} \frac{\vec{k}\vec{k}_0}{kk_0} - \varepsilon k k_0\right)}{\left(\varepsilon q_k + q_k^{(\varepsilon)}\right)\left(\varepsilon q_{k_0} + q_{k_0}^{(\varepsilon)}\right)} \quad \text{(A11)}$$

where ε is a complex dielectric constant of sea water, q_k is given by (A2), and

$$q_k^{(\varepsilon)} = \sqrt{\varepsilon(\omega/c)^2 - k^2} \quad \text{(A12)}$$

is a vertical projection of the wave vector in the sea water, with $Im\ q_k^{(\varepsilon)} > 0$. Explicit expressions for B for EM waves of other polarizations can be found in [30].

For monostatic radar, locations of the transmitting and receiving antennas are the same. The specularly reflected component can be removed by the time gating and will be omitted in what follows [see also the comment made after (19)]. Substituting (A8) into (A6) gives

$$\begin{aligned}\Psi_{\rm rec}(\vec{r}_0,z_0) &= \frac{c}{\pi\omega}\int d\vec{k}_0 d\vec{k} d_{tr}(\vec{k}_0)\,d_{\rm rec}(\vec{k})\,B(\vec{k},\vec{k}_0) \\ &\quad\times e^{i(\vec{k}-\vec{k}_0)\,\vec{r}_0 + i(q_k+q_{k_0})\,z_0}\hat{h}(\vec{k}-\vec{k}_0) \\ &= \frac{c}{\pi\omega}\int d\vec{\xi}\hat{h}(\vec{\xi})e^{i\vec{\xi}\vec{r}_0}\int d\vec{k}_0 d_{tr}(\vec{k}_0)\,d_{\rm rec}(\vec{k}_0+\vec{\xi}) \\ &\quad\times B(\vec{k}_0+\vec{\xi},\vec{k}_0)\,e^{i(q_{|\vec{k}_0+\vec{\xi}|}+q_{k_0})\,z_0}. \end{aligned} \quad \text{(A13)}$$

If $\omega z_0/c \gg 1$, the inner integral over $\vec{k}_0$ can be calculated using the stationary phase method. The stationary point $\vec{k}_0^{(st)}$ follows from

$$\frac{d}{d\vec{k}_0}(q_{|\vec{k}_0+\vec{\xi}|}+q_{k_0}) = -\frac{\vec{k}_0+\vec{\xi}}{q_{\left|\vec{k}_0+\vec{\xi}\right|}} - \frac{\vec{k}_0}{q_{k_0}} = 0 \quad \text{(A14)}$$

whence

$$\vec{k}_0^{(st)} = -\frac{1}{2}\vec{\xi}. \quad \text{(A15)}$$

The calculation of the determinant of the corresponding Hessian gives

$$\det\frac{\partial^2}{\partial k_{0i}\partial k_{0j}}\left(q_{|\vec{k}_0+\vec{\xi}|}+q_{k_0}\right)\Big|_{\vec{k}_0=-\vec{\xi}/2} = 4\frac{\omega^2}{c^2}\frac{1}{q_{\xi/2}^4} \quad \text{(A16)}$$

and the expression for the scattered field (A13) in the far zone becomes

$$\Psi_{\rm rec}(\vec{r}_0,z_0) = \int d\vec{\xi}e^{i\vec{\xi}\vec{r}_0+2iz_0q_{\xi/2}}D(\vec{\xi})\hat{h}(\vec{\xi}) \quad \text{(A17)}$$

where

$$D(\vec{\xi}) = i\frac{c^2}{\pi\omega^2 z_0}q_{\xi/2}^2 d_{tr}\left(-\frac{\vec{\xi}}{2}\right)\,d_{\rm rec}\left(\frac{\vec{\xi}}{2}\right)\,B\left(\frac{\vec{\xi}}{2},-\frac{\vec{\xi}}{2}\right). \quad \text{(A18)}$$

The physical meaning of (A17) is straightforward: each sinusoidal harmonic of the surface roughness with wave vector $\vec{\xi}$ scatters back the plane wave from the superposition of incident plane waves, which satisfies the Bragg scattering condition (A15). The exponential factor (A17) represents the phase of the plane wave, which it acquires propagating toward the sea surface and back, and $D(\vec{\xi})$ accounts for spherical spreading, directivity patterns of the transmitter and receiver, and polarization-dependent intensity of Bragg scattering represented by B. Since the first order of the small perturbation method is used, amplitude of the backscattered field is directly proportional to the amplitudes of the surface waves $\hat{h}(\vec{\xi})$.

Sea surface waves with the scales of meters and longer can be represented as a superposition of linear waves over time intervals of the order of 10 s. Thus, we have

$$h(\vec{r},t) = \int d\vec{k}a(\vec{k})e^{i\vec{k}\vec{r}-if(k)t} + c.c. \quad \text{(A19)}$$

where $a(\vec{k})$ are constant complex amplitudes of sea waves and $f(k) = \sqrt{gk}$ is the circular frequency of a sea wave with wave number k (the dispersion relation) and "$c.c.$" stands for complex conjugation. The field of sea surface elevation, h, is, of course, time-dependent. Since, however, speed of surface points, $\dot{h}$, is negligible as compared with the speed of light, expression (A19) can be directly used in (A17) with time t being treated as a parameter. This is the quasi-static approximation: for a given radar pulse sea surface is "frozen," and scattering proceeds from a snapshot of the sea surface.

For $\hat{h}(\vec{\xi})$ calculated at a time $t = t_0$ from (A10) and (A19), one finds

$$\hat{h}(\vec{\xi}) = a(\vec{\xi})e^{-if(\xi)t_0} + a^*(-\vec{\xi})e^{if(\xi)t_0}. \quad \text{(A20)}$$

Finally, substitution of (A20) into (A17) gives the following expression:

$$\Psi_{\rm rec}(\vec{r}_0,z_0,t_0) = \int d\vec{\xi}e^{i\vec{\xi}\vec{r}_0+2iz_0q_{\xi/2}}D(\vec{\xi}) \times[a(\vec{\xi})e^{-if(\xi)t_0} + a^*(-\vec{\xi})e^{if(\xi)t_0}]. \quad \text{(A21)}$$

Equation (A21) was obtained under the assumption that the point source given by (A3) has a unit amplitude. For this reason, $\Psi_{\rm rec}$ in (A21) corresponds to Ψ_n in (3).

ACKNOWLEDGMENT

The authors would like to thank the reviewers for their thorough reviews and valuable suggestions. They would also like to thank J. Toporkov for his constructive input, which led to revisions of some statements made in the original version of the paper.

REFERENCES

[1] D. E. Barrick, "Remote sensing of sea state by radar," in *Remote Sensing of the Troposphere*, V. E. Derr, Ed., U.S. Government Printing Office, Washington, DC: 1972, Ch. 12, pp. 1–46.

[2] L. R. Wyatt, "The ocean wave directional spectrum," *Oceanography*, vol. 10, no. 2, pp. 85–89, 1997.

[3] J. D. Paduan and H. C. Graber, "Introduction to high-frequency radar: Reality and myth," *Oceanography*, vol. 10, no. 2, pp. 36–39, 1997.

[4] C. C. Teague, J. F. Vesecky, and D. M. Fernandez, "HF radar instruments, past to present," *Oceanography*, vol. 10, no. 2, pp. 40–44, 1997.

[5] K.-W. Gurgel, G. Antonischki, H.-H. Essen, and T. Schlick, "Wellen radar (WERA): A new ground-wave HF radar for ocean remote sensing," *Coast. Eng.*, vol. 37, nos. 3–4, pp. 219–234, 1999.

[6] B. Lipa and B. Nyden, "Directional wave information from the SeaSonde," *IEEE J. Ocean. Eng.*, vol. 30, no. 1, pp. 221–231, Jan. 2005.

[7] I. R. Young, W. Rosenthal, and F. Ziemer, "A three-dimensional analysis of marine radar images for the determination of ocean wave directionality and surface currents," *J. Geophys. Res.*, vol. 90, no. C1, pp. 1049–1059, 1985.

[8] F. C. Jackson, W. T. Walton, and P. L. Baker, "Aircraft and satellite measurement of ocean wave directional spectra using scanning-beam microwave radars," *J. Geophys. Res.*, vol. 90, no. C1, pp. 987–1004, 1985, doi: 10.1029/JC090iC01p00987.

[9] R. C. Beal *et al.*, "A comparison of SIR-B directional ocean wave spectra with aircraft scanning radar spectra," *Science*, vol. 232, no. 4757, pp. 1531–1535, 1986.

[10] E. J. Walsh *et al.*, "Hurricane directional wave spectrum spatial variation at landfall," *J. Phys. Oceanogr.*, vol. 32, no. 6, pp. 1667–1684, 2002.

[11] W. R. Alpers, D. B. Ross, and C. L. Rufenach, "On the detectability of ocean surface waves by real and synthetic aperture radar," *J. Geophys. Res.*, vol. 86, no. C7, pp. 6481–6498, 1981.

[12] K. Hasselmann *et al.*, "Theory of synthetic aperture radar ocean imaging: A MARSEN view," *J. Geophys. Res.*, vol. 90, no. C3, pp. 4659–4686, 1985.

[13] P. A. E. M. Janssen, "On the nonlinear mapping of a surface gravity wave spectrum into a SAR image spectrum and freak wave detection," in *Proc. Envisat Symp.*, Montreux, Switzerland, pp. 1–6, Apr. 2007.

[14] J. Schulz-Stellenfleth, T. König, and S. Lehner, "An empirical approach for the retrieval of integral ocean wave parameters from synthetic aperture radar data," *J. Geophys. Res.*, vol. 112, no. C3, p. C03019, 2007, doi: 10.1029/2006JC003970.

[15] E. J. Walsh, I. PopStefanija, S. Y. Matrosov, J. Zhang, E. Uhlhorn, and B. Klotz, "Airborne rain-rate measurement with a wide-swath radar altimeter," *J. Atmos. Ocean. Technol.*, vol. 31, no. 4, pp. 860–875, 2014.

[16] D. D. Crombie, "Doppler spectrum of sea echo at 13.56 Mc./s.," *Nature*, vol. 175, pp. 681–682, Apr. 1955.

[17] D. E. Barrick, "First-order theory and analysis of MF/HF/VHF scatter from the sea," *IEEE Trans. Antennas Propag.*, vol. AP-20, no. 1, pp. 2–10, Jan. 1972.

[18] J. V. Toporkov and M. A. Sletten, "Numerical simulations and analysis of wide-band range-resolved HF backscatter from evolving ocean-like surfaces," *IEEE Trans. Geosci. Remote Sens.*, vol. 50, no. 8, pp. 2986–3003, Aug. 2012.

[19] G. Franceschetti and R. Lanari, *Synthetic Aperture Radar Processing*. Boca Raton, FL, USA: CRC Press, 1999.

[20] L. M. H. Ulander, H. Hellsten, and G. Stenstrom, "Synthetic-aperture radar processing using fast factorized back-projection," *IEEE Trans. Aerosp. Electron. Syst.*, vol. 39, no. 3, pp. 760–776, Jul. 2003.

[21] A. Reigber *et al.*, "Very-high-resolution airborne synthetic aperture radar imaging: Signal processing and applications," *Proc. IEEE*, vol. 101, no. 3, pp. 759–783, Mar. 2013.

[22] M. Sun, J. Xie, Z. Ji, and W. Cai, "Remote sensing of ocean surface wind direction with shipborne high frequency surface wave radar," in *Proc. IEEE Radar Conf.*, May 2015, pp. 39–44.

[23] S. R. J. Axelsson, "Frequency and azimuthal variations of radar cross section and their influence upon low-frequency SAR imaging," *IEEE Trans. Geosci. Remote Sens.*, vol. 33, no. 5, pp. 1258–1265, Sep. 1995.

[24] H. Hellsten, L. M. H. Ulander, A. Gustavsson, and B. Larsson, "Development of VHF CARABAS II SAR," *Proc. SPIE*, vol. 2747, pp. 48–60, Jun. 1996.

[25] L. M. H. Ulander *et al.*, "Development of the ultra-wideband LORA SAR operating in the VHF/UHF-band," in *Proc. IEEE Int. Geosci. Remote Sens. Symp. (IGARSS)*, vol. 7. Jul. 2003, pp. 4268–4270.

[26] V. Shteinshleiger, A. Dzenkevich, G. Misezhnikov, and L. Mel'nikov, "On the possibility of designing a high-resolution space-borne VHF-band SAR for remote sensing of the earth," in *Proc. EUSAR*, 1996, vol. 96, pp. 321–324.

[27] V. B. Shteinshleiger, A. V. Dzenkevich, V. Y. Manakov, L. Y. Melnikov, and G. S. Misezhnikov, "Obtaining high resolution in transionospheric spaceborne VHF-band SAR for Earth remote sensing," in *Proc. IEE Conf. Radar*, Oct. 1997, pp. 268–272, doi: 10.1049/cp:19971676.

[28] L. M. H. Ulander *et al.*, "Bistatic VHF/UHF-band airborne SAR experiment," in *Proc. IET Int. Conf. Radar Syst. (Radar)*, 2012, pp. 1–6.

[29] A. G. Voronovich, *Wave Scattering From Rough Surfaces*, 2nd ed. Berlin, Germany: Springer, 1999.

[30] A. G. Voronovich and V. U. Zavorotny, "Theoretical model for scattering of radar signals in K_u- and C-bands from a rough sea surface with breaking waves," *Waves Random Media*, vol. 11, no. 3, pp. 247–269, 2001.

Alexander G. Voronovich received the M.Sc. Degree in physics and the Ph.D. degree in theoretical and mathematical physics from the Moscow Institute of Physics and Technology, Moscow, Russia, in 1972 and 1975, respectively, and the Dr.Sc. degree in theoretical and mathematical physics from the Acoustical Institute, Moscow, in 1988.

From 1975 to 1979, he was a Junior Research Scientist with the Acoustical Institute. In 1980, he joined P. P. Shirshov Institute of Oceanology, Moscow, as a Senior Research Scientist, and became a Professor of Physics with the Moscow Institute of Physics and Technology, in 1991. From 1989 to 1993, he was a Head of the Laboratory of Acoustical Waves Propagation in the Ocean, P. P. Shirshov Institute of Oceanology. He is currently an Oceanographer with the Earth System Research Laboratory, National Oceanic and Atmospheric Administration, Boulder, CO, USA. His research interests include wave scattering from rough surfaces, ocean acoustics, geophysical hydrodynamics, internal waves, and linear and nonlinear theory of wave propagation.

Dr. Voronovich is a Fellow of the Acoustical Society of America.

Valery U. Zavorotny (M'01–SM'03–F'10) received the M.Sc. degree in radio physics from Gorky State University, Gorky, Russia, in 1971, and the Ph.D. degree in physics and mathematics from the Institute of Atmospheric Physics, USSR Academy of Sciences, Moscow, Russia, in 1979.

From 1971 to 1990, he was with the Institute of Atmospheric Physics, USSR Academy of Sciences. In 1990, he joined the Lebedev Physical Institute, Moscow. He is currently a Physicist with the Earth System Research Laboratory, National Oceanic and Atmospheric Administration, Boulder, CO, USA. His research interests include the theory of wave scattering from rough surfaces, ocean and land remote sensing applications using radar, and global navigation satellite system reflection techniques.

Dr. Zavorotny is a member of the American Geophysical Union and Commission F of the U.S. National Committee of URSI. He is also a member of the NASA Cyclone Global Navigation Satellite System Mission Science Team.